Large Eddy Simulation of natural exhaustion effect in a corridor fire using vertical duct

Imen Ben Abdellaziz[#1, *1], Mourad Bouterra[#2], Afif El Cafsi[#3]

[#1]*Physics Department, Laboratory of Energetics, Thermal and Mass Transfers (LETTM), University of Tunis El Manar, Faculty of Sciences of Tunis, El Manar II, 2092, Tunis, Tunisia.*

[*1]*Hafr Al Batin University, Kingdom of Saudi Arabia*

benabdellazizimen@gmail.com, Mourad.Bouterra@gmail.com;elafif.k@gmail.com

***Abstract*— Both numerical and theoretical study on a vertical exhaustion efficiency in a corridor fire and state stratification behaviours of the smoke under different duct sections and heights were conducted. Results show that the mixing process, the stack effect and the plug-holing are the dominating factors on the natural ventilation efficiency. There exists an optimal duct section, such as the hot smoke will be adhered to the upstream and the downstream walls of the duct. The 2D flow pattern in near region could be used to improve the efficiency process of the natural disastrous smoke exhaustion. In this case we obtained the maximum efficiency at about 82.1 %. It was found also that during the plug-holing effect, the smoke layer is completely destroyed were the downstream layer is predicted by the stratification parameter evolution. The temperature at upper height approachs to the lower temperature layer and the $''S_{nw,dow}''$ shows an important decreasing ($''S_{nw,dow} < 1''$). So, the stratification become unstable. This work is beneficial for safety evaluation and optimization design of tunnel safety engineering using natural exhausting duct effect.**

***Keywords*—** Tunnel fires, natural smoke exhaustion, LES, Stratification.

I. INTRODUCTION

Several catastrophic fires have occurred in the past decade. Examples of such fires include the corridor-like structures [1-3] and other include the tunnel fire. Generally, a tunnel fire is a complex flow phenomenon that depends on many factors as the geometry of tunnel and the ventilation system. It can be considered as a possible idea of applying similar a model to the corridor modeling structure. In case of tunnel fire, the hazardous gas diffuses and spreads widely over this confined space, causing a disastrous suffocations and leading to catastrophic loss of human lives. Statistics have shown that smoke is the most hazardous factor in tunnel fires as it was even the cause of dramatic events such as the case of the Mont-Blanc (39 deceases), the Tauern (11 decades) and the Gotthard (12 decades) tunnels [4]. The propagation of smoke combustion is likely depending on the ventilation systems that are set up in the tunnel. Tunnel ventilation systems fall into two main categories. The natural ventilation and the mechanical ventilation. The design of mechanical ventilation system needs more place for the installation and increases the operation of the utility bills. However, the natural ventilation using vertical duct consumes less power in addition of naturally-occurring forces employment.

In tunnel fire research, the buoyancy-driven smoke flow layering length beneath the ceiling by point extraction and longitudinal ventilation combination [5], the ventilation performance realization by mechanical exhaust system [6, 7] have been widely studied. The temperature distribution and stratification of smoke in a tunnel at 1-D propagation phase with variation of

ISSN: 2961-6603

the ventilation strategy are conducted by Kalech et al. [8]. They found that in case of a transversal ventilation strategy, the smoke layer is maintained below the ceiling, between the two openings A and D, at height 20% of h from the ceiling. The smoke flow is perfectly stratified. Vauquelin and Mégret [9], have investigated experimentally the smoke extraction of a transverse ventilation system. The tunnel is equipped with two ducts located one on either side of a fire source in order to study the influence of their location and their shape on the exhaust system efficiency in a first step, then the effect of the fire heat release. They conclude that the efficiency of 100 % is reached for 10 and 20 MW.

With the methods development used to design a ventilation system, the benefit characteristic of the natural ventilation system with vertical duct has become more and more attractive. The position of ventilation system can be conducted using full-scale tests which require very large.

Ji et al. [10], were analyzed numerically by Large Eddy Simulation (LES), the influence of cross-sectional area and aspect ratio of duct on natural ventilation. He demonstrated that when the cross-sectional aspect ratio increases to a certain value, the hot smoke will be adhered to the upstream wall of the duct that will be exhausted through the upstream region and this latter is predicted by using the 2D flow pattern interpretation. Zhong et al. [11] numerically analyzed (by the code Fire Dynamic Simulator (FDS.5)) the smoke flow characteristics of a road tunnel fire under the combined function of a longitudinal wind and stack effect of duct. The effect of vertical duct height on natural ventilation is investigated experimentally by Ji et al. [3], two special phenomena plug-holing and turbulent boundary-layer-separation was influenced by the effect of smoke exhaustion. He et al. 2023 [12] studied the behaviour of air supply in tunnels with multiple vertical shafts during fire incidents, focusing on natural ventilation dynamics. Result show that the position of the smoke front significantly influences the direction and flow rate of gases during fire development. The mass flow rate of air supply during the stable fire development stage is influenced by the geometric size and positioning of vertical shafts, with shafts closer to the fire source exhibiting higher air flow rates.

Currently, many studies have conducted a particular research on stratification state based on natural exhaustion effect by vertical duct. The buoyant flow stratification behaviour is studied by Tang et al. [13] based on instability criterion for the smoke layer in tunnel fire with complex combination of longitudinal ventilation and ceiling extraction. The Richardson number is predicted where the buoyancy and inertial forces are the two important factors influencing the buoyancy stratification. They found that the stratification became unstable with a strong mixing flow when $(Ri < 1.4 \; or \; Fr > 0.8)$. The smoke stratification behaviors caused by fire and outdoor wind is experimentally predicted by Huang and Li [14]. In order to to describe the layering properties, Froude number was proposed and a correlation for the stratification characteristic of smoke was defined as follow:

$$\frac{\Delta T_{cf}}{\Delta T_{avg}} = 70.43 \; exp\left(-\left(\frac{Fr+4.357}{2.427}\right)^2\right) \qquad (1)$$

In all the previously cited results, the parametric conditions of a vertical duct system in the tunnel roof on natural ventilation efficiency have not been completely addressed and discussed. Therefore, in order to investigate the natural ventilation efficiency using vertical duct, the method of Large Eddy Simulation (LES) was adopted and two scenarios were stimulated respectively: The variation of the duct section and the duct height. The term of efficiency is calculated first with the flow field pattern description. Then, a criterion for the stratification state is also studied were critical conditions to maintain the downstream smoke stratification are numerically analyzed. The objective of this research is to focus on the smoke exhaustion efficiency by natural ventilation and improve the best duct parametrical condition to obtain an excellent performance for the vertical duct control respecting the state stratification of the smoke based on a new criterion for the smoke stability control.

ISSN: 2961-6603

II. NUMERICAL TECHNIQUES

A. Physical Model Setup

The physical domain under investigation is shown in Fig. 1, which simulated a fire in a tunnel and consisted of two principal units, the tunnel and the duct (Fig. 1 (b)). For the realization of their numerical experiments, the authors used the geometry shown in fig. 1 [3]. Initially, we follow the same pattern with the same boundary conditions for the comparison of results. The experiments were conducted in a small-scale model with a ratio of 1:6 [3]. The tunnel is 6 m long, 2 m wide and 0.9 m high. The duct is set up 4.2 m away from the left side (Fig. 1) and is topped vertically in the ceiling with a size of (0.3 m, 0.3 m, 0.8 m). The internal lining of the tunnel and duct are specified as ‘‘CONCRETE’’. The physical properties of this material are specified in the FDS model based on data provided by FDS. The top of the duct and tunnel entrance are naturally open, without initial speed. The initial temperature of tunnel wall is set to be 20 °C. Fire is simulated by a source placed at 1.2 m (Fig. 1) away from the left opening of the tunnel. Fire power is determined by the command heat release rate per unit area “HRRPUA’’ provided in FDS. The dimension of the source of fire is $(0.2\ \mathrm{m} \times 0.2\ \mathrm{m})$ with a size HRR (The heat release rate of the fire) of 20.21 KW [3]. In this study, the HRRPUA is steady for all simulations.

Figure 1 (b) illustrates the duct provision in the tunnel ceiling and the schematic diagram of the model with FDS simulation is shown in Fig. 2. As it is shown in Fig. 2, the total area of the tunnel with the duct system, the “OPEN” boundary condition for the left direction of the tunnel and the fire source (with the color red) localization are very clearly illustrated by FDS simulation. Fig. 2 presents also the different transverse planes (with the color green) for several longitudinal displacements along the tunnel which are required to calculate the convective HRR in the upstream (the left direction of the source zone) and the downstream directions (the right direction of the source zone) of the source zone in addition the upstream (the left direction of the duct) and the downstream (the right direction of the duct) directions of the duct emplacement. The objective is to prove the efficiency of an exhaust duct (see part 3) by changing its geometry.

In order to investigate respectively, the influences of the duct section and height, we are simulated two series of fire-scenarios. First, we fixed the duct height as 0.8 m and we will be varied the section from 0.01 m^2 to 0.36 m^2. Second, the section is fixed 0.09 m^2 (0.3 * 0.3), then, the height is changed from 0.1 m to 1 m.

B. Fire Dynamics Simulator

The application of the computational fluid dynamics (CFD) technology to analyze problems involved in three-dimensional flows in tunnel fire [15] has become possible with the development of (CFD) and the advent of increasing computer power. CFD codes such as FDS was previously used for tunnel issues (fire and ventilation) [11]. The Fire Dynamics Simulator (FDS) [16, 17], developed at NIST (National Institute of Standards and Technology), USA, is a model of fire-driven fluid flow, coded for this work in Fortran input record and run from the command prompt. Its accuracy has been validated in many tests [18, 19]. The mathematical description refers to the FDS technical guide [17]. Based on the Hydrodynamic Model [16, 17], FDS solves

ISSN: 2961-6603

numerically a form of the Navier-Stokes equations appropriate for low speed, thermally-driven flow with an emphasis on smoke and heat transport from fires.

The turbulence model of FDS includes Direct Numerical Simulation (DNS) and Large Eddy Simulation (LES). In this study, we chose the LES model, due to its intensive user to simulate the problem of the tunnel fire and the development of the disaster smoke.

The Smagorinsky in LES simulation is flow dependent and sets as low as possible to maintain numerical stability. It has been optimized over a range from 0.1 to 0.25 for various flow fields [20]. Two points should be considered in the prediction of the smoke movement by LES [16, 17]: The fine enough grids and the suitable sub-grid model (SGM) on small eddies. The Sub-Grid-Model (SGM) which is applied in LES, is carried out by Smagorinsky [21]. The eddy viscosity is defined as the equilibrium between the energy production and dissipation (the small scales). The turbulent viscosity defined in FDS by [16,17]:

$$\mu_{LES} = \rho(c_s\Delta)^2[2\bar{S}_{ij} : \bar{S}_{ij} - \frac{2}{3}(\nabla.\bar{u})^2]^{1/2} \quad (2)$$

Where C_s is the empirical Smagorinsky constant, Δ is $(\delta x\delta y\delta z)^{1/3}$ and the term $\bar{S}$ consists of second-order spatial differences averaged at the grid centre.

The thermal conductivity k_{LES} and material diffusivity D_{LES} of the fluid are related to the viscosity μ_{LES} in term of the Prandtl and Schmidt numbers by:

$$k_{LES} = \frac{c_P\,\mu_{LES}}{Pr}, \qquad (\rho D)_{l,LES} = \frac{\mu_{LES}}{Sc} \quad (3a, 3b)$$

The numbers of Prandtl and Schmidt are assumed to be constant. The specific heat, C_p is taken to be that of the dominant species of the mixture [16, 17]. According to many validation works, the constants C_s, Pr and Sc are defaulted in FDS as 0.2, 0.2 and 0.5 [16], respectively. In our study, and in order to set these parameters, we tested many values. The 0.2 for the C_s number and 0.2 for the Pr number allowed for a fusty convergence of the model [11, 22].

The Courant-Friedrichs-Lewy (CFL) criterion is used in FDS for justifying numerical convergence. It is more important for large-scale calculations where the time step is constrained by the convective and diffusive transport speeds. So, the estimated velocities are tested at each time step to ensure that the CFL is satisfied via this condition [17]:

$$\delta t.\max\left(\frac{|U_{ijk}|}{\delta X}, \frac{|V_{ijk}|}{\delta Y}, \frac{|W_{ijk}|}{\delta Z}\right) \pi\ 1 \quad (4)$$

Where U_{ijk} , V_{ijk} and W_{ijk} are respectively the velocity vector in x, y and z-axis direction. δX , δY and δZ present the dimensions of the smallest grid cell in x, y and z direction.

The time step is eventually changed to a quasi-steady value when the fire burns steadily. The numerical analysis results are sensitive to the grid size used.

C. Validation of Results

FDS is a fire spreading and smoke transport simulation software widely used in tunnel, corridor and stations. Engineers must have a good understanding on the physics behind, so that results can be judged appropriately. Therefore, before making the numerical simulation, it is necessary to make the validation of the numerical code and to analyze the mesh nature because it presents a key parameter to be considered. Also, it is necessary to make a sufficiently fine mesh in order to obtain a more

ISSN: 2961-6603

accuracy results. However, an excessively fine mesh leads to a long time step. Certain rules are applied here in terms of the sizes and the shapes of the cells in order to limit the numerical errors.

The $\frac{D^*}{\delta X}$ criterion has been widely used for assessing the grid resolution [16, 23]. The characteristic length of D^* is calculated by:

$$\left(\frac{Q}{\rho_\infty c_p T_\infty \sqrt{g}}\right)^{2/5} \quad (5)$$

c_p is the specific heat capacity and $\dot{Q}$ is the heat release rate. The quantity $\frac{D^*}{\delta X}$ can be thought of as the number of computational cells spanning the characteristic diameter of the fire. According to a large number of domestic and foreign scholars, the values of $\frac{D^*}{\delta X}$ ranging from 4 to 16 give good simulation results [16, 24]. Also the grid size of the finest mesh for a 4 MW fire was calculated to be between 0.1 m and 0.4 m [25].

In this paper, four different mesh sizes ranging from 0.1–0.2 m are chosen for comparison. Figure 3 illustrates the distribution of the vertical temperature in the corridor with different grid sizes. It presents the confrontation of our numerical simulation to the experimental result [3]. It is very clear that with the mesh density increasing, the temperature curve trends to be uniform. The result of mesh (A) with 0.2 m is the lowest (A1). The numerical points are far from the experimental points. A2 is the higher curve, with 0.1 m mesh density. There is here more time consuming. The mesh with 0.187 m (A4) provide a good confrontation between the point measurements. A multi-mesh system (A3) with grid size of 0.2 m at the zone source and the duct-system and 0.187 m in the other regions, presents the best curve. There is more coincidence between the experimental and the numerical points. Also, less time consuming is obtained. Hence, we choose this multi-mesh system (A3).

It is very clear that in case of thermocouple tree at h = 0.85 m, the temperatures rise sharply from the ambient temperature to the values of (52 °C - 59 °C) at about 150 s. Then, it keeps stable at the range of (60 °C – 65°C) until 300 s. This latter can be explained by the fact that the upper part of the thermocouple is located in the smoke layer at the upper part of the tunnel. For example, we can notice that the temperature achieves at about 60°C at 300 s [3]. However, our numerical result finds out 64°C. A good agreement was obtained.

It can be conducted also from this Fig. 3 that the total time step is 300 s. The time step is eventually changed to a quasi-steady value when the fire burns steadily. The steady state corresponds to 180 s - 300 s. The regime is realized under this period. So, all our results are extracted and so examined in this time (between 180 s - 300 s).

III. NATURAL EXHAUSTING EFFICIENCY

In order to ameliorate the natural extraction process during tunnel fire, the separation interface between the tunnel and the exhaustion system should be reduced as little as possible. So, the amount of air which is penetrated into the smoke or drawn directly into the duct from the lower layer must be very small. In case of natural ventilation control, the 100% efficiency will be achieved only by increasing the convective heat release rate (convective HRR) of the smoke extract system. So, the convective HRR of smoke exhausted by the duct can be regarded as a key factor to judge if the natural ventilation process is effective.

Vauquelin and Mégret [9], defined the efficiency of an extract duct to characterize the transverse ventilation system. It constitutes the ratio of the extracted smoke VFR (Volume Flow Rate) to the produced smoke VFR and can be expressed as follows:

ISSN: 2961-6603

$$\varepsilon = \frac{Q_{es}}{Q_s} \quad (6)$$

In this study, a simple definition will be conducted for the design of the smoke exhausting effect. It has similar physical meaning with Vauquelin and Mégret application. However, there is an evidently new modification. The objective is to evaluate the natural performance effect of a vertical duct in a corridor fire.

The method is based on convective HRR calculation under different planes for several transversal displacements along the tunnel. Each plane is illustrated by a matrix for component of temperature and velocity calculation in the j and k direction (T_{jk} ,V_{jk}) as it is presented in Fig. 2.

The term of ''efficiency'' of the smoke exhaustion can be calculated through the following equation:

$$Ef = \frac{\mathrm{HRR}_{\mathrm{exh}}}{\mathrm{HRR}_{\mathrm{pro}}} \quad (7)$$

Were, $$HRR = \iint U\,[T - T_a]\,d\sigma = \sum_{jk} U_{jk}\left[T_{jk} - T_a\right]\Delta Y \Delta Z \quad (8)$$

The different quantities can be calculated are:

- The $\mathrm{HRR}_{\mathrm{pro\,(ups)}}$ is the produced HRR calculated in the upstream (the left direction of the zone source) direction.
- The $\mathrm{HRR}_{\mathrm{pro\,(dow)}}$is the produced HRR calculated in the downstream (the right direction of the zone source) direction.
- The $\mathrm{HRR}_{\mathrm{exh}}$ is the exhaust HRR calculated under the smoke vent (the limit area between the duct and the tunnel roof).
- The $\mathrm{HRR}_{\mathrm{rsd}}$ is the residual HRR calculated in the downstream direction of the duct location.

Where U_{jk} and T_{jk} are the longitudinal component velocity and the temperature respectively calculated in each plane, T_a is the ambient temperature and σ is the cross-section area for each considered plane.

For each simulated case, we kept the same measurement point to calculate the $\mathrm{HRR}_{\mathrm{pro\,(ups)}}$ (1.7 m), and the $\mathrm{HRR}_{\mathrm{pro\,(dow)}}$ (3.85 m), however, the $\mathrm{HRR}_{\mathrm{exh}}$ and the $\mathrm{HRR}_{\mathrm{rsd}}$ will be changed from one case to another.

So, for the two different fire scenarios, the duct efficiency is determined depending on the ($\mathrm{HRR}_{\mathrm{exh}}$) and is calculated using the Eq. 10.

IV. RESULTS AND DISCUSSIONS

A. Influence of the Duct Section

1) Exhaust efficiency of duct

Figure 4 presents the efficiency of the duct at different cross-sections of 0.01 m^2, 0.04 m^2, 0.09 m^2, 0.16 m^2, 0.25 m^2 and 0.36 m^2. From the figure, we can observe that the efficiency increases with the increase of the duct section. This rising features an exponential behavior. This is well observed in the study of Vauquelin and Mégret [9] in order to investigate the efficiency and the relative VFR for different duct locations. It is very clear that the maximum efficiency is reached in case of the bigger duct (s = 0.36 m^2) and it is far from being obtained (82.1 %). It can be noticed that there exists a low entrainment effect of air fresh through the limit area between the tunnel roof and the duct bottom. This can be explained by the fact that when the horizontal velocity of the smoke flowing into the duct becomes higher, the stack effect causes a weaker induction of a vertical

ISSN: 2961-6603

inertia force and the smoke flow becomes controlled by the horizontal component. As a result, a small quantity of fresh air will be extracted from the duct were the active smoke exhausting region can slightly decrease. Consequently, 4/5 of the total efficiency of the smoke exhausting is obtained.

2) Flow field pattern

In this sub-section, we will intend to examine the flow field pattern in the tunnel and the duct in order to improve the phenomena that are occurred along the smoke exhausting effect with the duct section variation and caused the decrease of the natural smoke extraction process.

Figure 5 shows the distribution of the temperature for three different section (s = 0.04 m^2, s = 0.16 m^2, and s = 0.36 m^2) in tunnel and the duct were the left side presents the duct-system.

As shown in Figs.5(a), when the disturbance on smoke layer interface starts to break the stability of the smoke induced by the smaller vertical inertia force effect, a bit quantity of fresh air mixed into the smoke layer and a very small hollow (leakage area) under the smoke vent appears. The particles of smoke found a big problem to enter in to the duct because the upper point of leakage region is still smaller than the installing point in the downward ceiling part. The only small quantities that can include it are founded so closed to each other and will be blocked in the bottom and the middle section. The smoke is unable to separate from this region and then to exhaust through the duct section of 0.04 m^2. So, this is the cause of the smoke exhausting inefficiency in this case as it is shown in Fig.4. However, in case with duct section larger than 0.04 m^2, and under the average driving effect of the vertical inertia force, it is very clear that the highest points of the smoke-hollow (hollow in the smoke layer) appear more clearly (Figs.5(b) and 5(c)). These leakage areas are circulated with the color red in Fig. 5 and namely “the sunken areas”. The lower limit layer starts to interact with the upper area of the tunnel center where the flow speed increases rapidly with the duct section increasing and leads to the mixture process between the two species. When the smoke layer thickness below duct weakness, the highest point enters into the middle of the duct and the mixed fresh air with smoke is drawn into the duct bottom. As it is shown in Fig.5(b) and in the lower part of the duct section of 0.16 m^2, the temperature in the left region from the tunnel ceiling and the lower duct area are about 61°C and 60°C respectively. There exists also an area where the thermal field reaches the 39°C value in the right region of the tunnel roof. However, the temperature keeps the value of 36°C in the lower duct from the right area. We can easily confirm an entrainment of a proportion of fresh air from the tunnel center into the right duct region which will be the cause of the temperature decrease in this area. Consequently, we obtain an average smoke exhausting efficiency in case of the average duct section (Fig. 4 and Fig.5(b)).

As shown in Fig.5(c), the temperature at the ceiling level is almost equal to that at the duct bottom. For example, we can notice that the temperature reaches 61°C and 39°C in the left and in the right parts of the sunken area, respectively (case for S = 0.36 m^2). The lower part of the duct is also characterized by a similarity from the thermal field (61°C in the left and 39°C in the right sides). It is very clear that the smoke layer stratification is stable under the duct because there is a thicker smoke layer and the horizontal inertia force is high. That stability limits the mixed air penetration into the smoke layer from the left and the right direction and avoids the occurrence of the stack effect. However, under the action of the weak vertical disturbance, the mixture process becomes a bit stronger due to the smoke exhausting of the duct, and a portion of fresh air will be flowing into the duct center. An amount of air is exhausted through it and the other part remains stable between the thicker smoke layers in the medium. The rest keep spreading along the tunnel ceiling. Therefore, the smoke efficiency is relatively large in this case (See Fig.4).

ISSN: 2961-6603

So, when the higher hot smoke flows inside the duct without mixture with cold air (both the left and the right direction of the duct), it illustrates the shape of the adhered behavior of spill plume. It is similar to the adhered form of spill plume in big region of building. It can be regarded as the 2D flow pattern in near region.

Therefore, various cross-sections of duct issue in tunnel roof have been envisaged and have obvious influence on the flow field pattern behavior and natural ventilation performance of the duct. A small duct section will inhibit the smoke exhausting effect process, resulting in poor natural ventilation performance. With a medium duct section, we achieve the 60 %. While the duct with a large section, will bring a better exhaust effect. However, the 100 % of smoke exhausting process is not achieved because of the mixing phenomena emergence which leads to the hot smoke dilution.

B. Influence of the Duct Height

1) Exhaust efficiency of duct

Figure 6 shows the duct efficiency for different duct height. It can be observed that the efficiency seems to be varied linearly with the vertical height and slightly increased with the duct height increases. For the duct height bellow 0.7 m, the efficiency does not exceed the 36 %, indicating that the exhaust smoke efficiency based on height vertical duct below 0.7 m is not significant. When the duct reaches the height of 1 m, we obtained the maximum percentage (62.35 %) and the efficiency seems to be with an average value. It is very clear that the flow motion is controlled by the vertical inertia force of the smoke. The smoke layer interface is totally broken and a lot of fresh air can easily draw through the larger duct. So, the flowing smoke to the duct weakness progressively. The reason is that when the vertical inertia force is large, the fresh air beneath smoke layer is directly exhausted and plug-holing occurs, resulting in the duct efficiency reduction.

In the next part, we will prove the process of the plug-holing (based on the flow pattern analyses) and its impact on the smoke exhausting effect (reduction of the smoke exhausting effect).

2) Flow field pattern

In this sub-section, we will interest to plot the same contour as it is discussed in part 4.1.2, however with respecting the duct height variation. The temperature contours in the tunnel are located at a fixed plan (Y = 1) along the total length (X: 0 m – 6 m) and height (Z: 0 m - 0.9 m). In the duct, they are located at a fixed plan (Y = 1) along the total length (4.2 m – 4.5 m). However, the height is varied.

Figure 7 presents the distribution of temperature for different duct heights under S = 0.09 m^2. Results for duct heights of 0.4 m, 0.6 m, 0.8 m and 1 m are selected here. As it is observed in Figs. 7(a) and 7(b), the hollow form and the height of the sunken point progressively rises with the increasing of the duct height. When the height is 0.4 m, a weak vertical stream of air appears at the medium duct level where the temperature is about 24°C. However, it seems at about 29 °C at the top of the duct level. For H = 0.6 m, the limit area of the smoke layer interacts with the center area of the tunnel. The sunken area appears more again were a secondary vertical stream of air emerges progressively. In this case the smoke is naturally exhausted from the upstream and the downstream direction of the duct along the penetration effect. This exhausting is predicted as an adhered behavior of spill plume as it is presented in part 4.2.1. With the duct height increase, Figs.7(c) and 7(d) show that the disturbances on smoke layer interface are strong and the intensity of vertical stack effect involved by the current of toxic gas from the roof of tunnel into the duct-system is gradually increased. The smoke layer under the duct- tunnel contact becomes very thin and the stratification is broken. When a strong “sunken area” appears (a large hollow along the smoke layer) and the thickness of smoke

ISSN: 2961-6603

layer under the contact area decreases to 0, the apex of the depression enters into the duct and the plug-holing occurs immediately, i.e. the fresh air is drawn directly into the duct from the lower area.

Fig.7(c) indicates the presence of two vertical air-streams which spread along the duct top and promote the weakness of the adhered spill plumes. There exists an area in the duct bottom were the temperature is about 25°C and about 36°C in the top area. In Fig.7(d), the two vertical air-streams start to interact with each other at the upper part of the duct where the downstream adhered spill plume weakens more once again. Therefore, a lot of air is easily exhausted by the duct.

Thus, we can conclude that the flow pattern with duct height variation is immediately determined with the combined function of the assumption of 2D flow pattern in near region and the two vertical air-streams. These two effects are defined to improve the phenomenon of natural smoke extraction process in case of a vertical duct provision in the tunnel ceiling after the entrainment observed through the upstream and the downstream directions.

C. Smoke Stratification State

Smoke stratification is an important issue for evacuation and fire fighting in tunnel fires. If the smoke stratification in a tunnel section dissolves, tunnel users in this region could be in great danger. In no ventilation conditions by vertical duct-system, smoke exists on both sides of the fire, and good stratification could exist at the early stages. In the presence of natural duct provision, different mechanisms can disturb the stability of the smoke stratification as the mixing and the plug-holing effects which will be decrease the performance of the exhausting-duct. An empirical model for the smoke stratification in tunnels is studied by Demouge [26]. He presents the theory of the stratification state based on temperature distribution and he defined a stratification parameter as follow:

$$S = \frac{T_{ac} - T_{af}}{T_{avg} - T_0} \tag{9}$$

Where T_{ac} is the temperature of fluid at the hot layer level, T_{af} is the temperature at the cold layer level, T_{avg} is the average temperature and T_0 is the ambient temperature. He prove that the stratification parameter is a key factor to judge if the smoke stratification is stable and the critical condition to determine the stable smoke stratification is $S > 1.1$.

In this study, a new model of the stratification parameter is conducted. This model is based on temperature calculation at a level height of the person and the exactely layers disposition of the fresh air and the dangerous smoke. From this point of view, the temperature variation as a function of the tunnel height for the duct height of 0. 4 m is presented in Fig.8. We can easily confirm from this figure there exist two layers. The first layer constitutes the fresh air. It is located between 0 m and 0.73 m heights. The second layer presents the hot smoke. It appears under the ceiling between the height levels of 0.73 m and 0.89 m. This parameter is defined as follow:

$$S_{nw} = \frac{T_{ul,avg} - T_{ll,avg}}{T_{avg} - T_0} \tag{10}$$

Where $T_{ul,avg}$ is the average temperature calculated in the hot layer between the height level of 0.73 m and 0.89 m. It is defined as bellow:

$$T_{ul,avg} = \iint \left[T - T_{inrf}\right] \, d\sigma = \sum_{jk} \left[T_{jk} - T_{inrf}\right] \Delta Y \Delta Z \tag{11}$$

$T_{ll,avg}$ is the average temperature calculated in the lower layer between the ground and 0.73 m height. It is defined as bellow:

$$T_{ll,avg} = \iint \left[T - T_0\right] \, d\sigma = \sum_{jk} \left[T_{jk} - T_0\right] \Delta Y \Delta Z \tag{12}$$

ISSN: 2961-6603

T_{jk} is the lonjitudinal component temperature calculated in each layer and σ is the cross-section of each considered upstream and downstream layer. T_{inrf} is the longitudinal component temperature calculated in the interface zone at 0.73 m. It constitute the temperature transformation for the downward state to the upward state. T_{avrg} presents the average temperature calculated along the two hot and cold layers. T_0 is the ambient temperature.

Figure.9 shows the relationship of $\frac{\Delta T_{ul,ll}}{\Delta T_{ul,o}}$ and S_{nw}. The domain can be divided in to two regions. $\frac{\Delta T_{ul,ll}}{\Delta T_{ul,o}}$ increased firstly and then stabilized with increasing S_{nw}. When S_{nw} > 1.1, $\frac{\Delta T_{ul,ll}}{\Delta T_{ul,o}}$ maintained as 1 indicating that is an interface between region 1 and region 2. The mean temperature for the lower layer of the corridor was approximately equal to the ambient temperature. The stratification is obvious, and the stratification state is in Region 1. Otherwise, the stratification is unclear, and the stratification state is in Region 2.

The distribution of the stratification parameter $''S_{nw}''$ in the upstream $''S_{nw,up}''$ and the downstream $''S_{nw,dow}''$ directions of the duct is shown in Fig.10 for three different duct sections (0.04 m^2, 0.16 m^2 and 0.36 m^2). It can be observed that while the section increased, the $''S_{nw,up}''$ increased significantly. It seems to be greater than 1.1. This result indicate that the smoke stratification is clear. In the downstream direction, the stratification is stable for the smaller duct since $''S_{nw,dow}''$ is greater than 1.1. With the increase of the duct section, the distribution of $''S_{nw,dow}''$ decays and the degree of stratification decreases significantly. This is because the mixing of hot smoke and cold air is important. For example, when s = 0.01 m^2 and for X/H = 6.5, $S_{nw} = 1$. For the largest cross section, the stratification of smoke became more disordered because $''S_{nw,dow}''$ seems to be less than 1.1. We take for example the case of the dimension less length of the tunnel is equal to 6.6, $S_{nw} = 0.8$, which might due to the continuous heat loss from smoke to the surroundings during the process of longitudinal spread, resulting in lower smoke temperature. So, the smoke stratification is unclear.

The distribution of the stratification parameter $''S_{nw}''$ in the upstream and the downstream direction of the duct is shown in Fig.11 respecting the variation of the duct height. The height level of 0.4 m, 0.6 m, 0.8 m and 1 m are selected here. Result show that the smoke stratification was stable in the upstream direction (Fig.11a) of the duct for all the listed tests since $''S_{nw,up}''$ is greater than 1.1. This is because the mixing of hot smoke and cold air is lower and a small part of the surrounding air is entrained into the duct upstream. With the particles-diffusion beginning and the entrainment upstream, the mixing process increases and the smoke layer stability decreases as it is shown in the part (4.1). It is clearly seen that the smoke stable-stratification in the downstream direction of the duct becomes shorter as the duct height increasing. Fig.11b reveals that for H = 0.4 m and when $\frac{X}{H} \in [5.25 - 5.6]$, the $''S_{nw,dow}''$ seems to be above the critical value were the stratification is clear. Then, it decreased significantly in the range from 5.7 to 6.7 of the less dimension $\frac{X}{H}$. It can be predicted that due to the longitudinal decay of the smoke temperature after a certain distance from the fire source, the $''S_{nw,dow}''$ is bound to fall below 1.1. At this time, the smoke stratification state will change from Region I to Region II. With the increase of the duct height (H = 0.6, H = 0.8), the major point of the $''S_{nw,dow}''$ seems to be below 1.1 indicating that the stratification was destroyed. For the case with the higher duct (H = 1 m), the $''S_{nw,dow}''$ shows an important decreasing trend along the longitudinal less dimension of the length, which might due to the directly entrainment of the ambient air during the plug-holing effect. The temperature at upper

ISSN: 2961-6603

height, approaches to the lower temperature layer and the smoke layer is completely destroyed. So, the smoke layer stratification became unstable.

V. CONCLUSIONS

In this parametrical study, a set of numerical simulations were conducted to investigate the effect of the section and the height of a vertical duct system issue at the ceiling projection on natural smoke extraction efficiency in a corridor fires with Large Eddy simulation (LES). The analysis of these results has provided the following conclusions:

The duct height constitutes an essential factor to be considered. When the duct is very low, it becomes unable to exhaust the maximum smoke outlet; leading to a poor natural ventilation. With the height of duct increase, a stronger stack effect is formed. The reason is that when the vertical component of inertia force is large, the fresh air in the superficial region is immediately extracted and the phenomenon of plug-holing occurs. So, the natural smoke extraction is inefficient.

However, the section of the duct presents the major factor to achieve a better performance for natural ventilation. Evidently, the total efficiency is not reached even for the greater duct. This is the cause of the mixing process producing and the drawing effect of the diluted gas into the duct bottom. The weak vertical inertia force acts to ameliorate the indirectly dilution discharging of the smoke with the air throw the upper part of the duct, leading to a smoke exhausting decrease and consequently the efficiency of natural extraction process reduction.

So, for achieving an extracting HRR efficiency and consequently a natural ventilation performance, it must be used with precaution and alternatively a considerable duct section and height.

ISSN: 2961-6603

Figure and Figure Captions

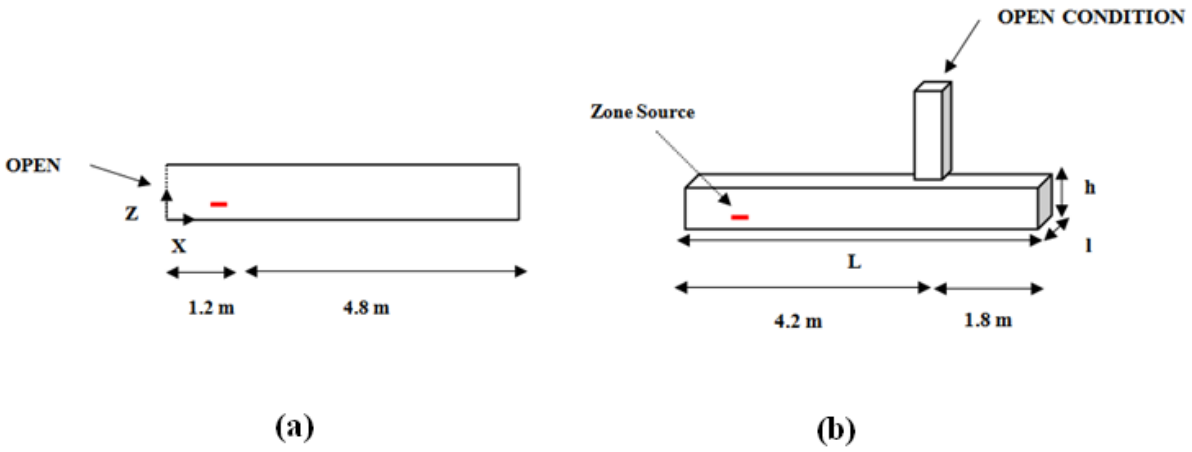

Fig. 1 The Schematic diagram of the model: (a) Corridor model; (b) Presence of the duct.

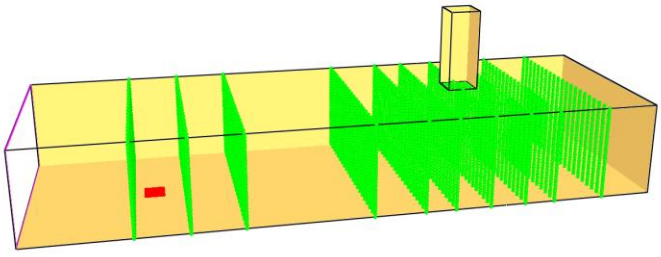

Fig. 2 Corridor topped by a duct system model established by FDS and the different transverse planes (The planes green are organized for the efficiency of the duct calculation) for several longitudinal X-displacements, with duct dimension of (0.3 m,0.3 m,0.8 m).

ISSN: 2961-6603

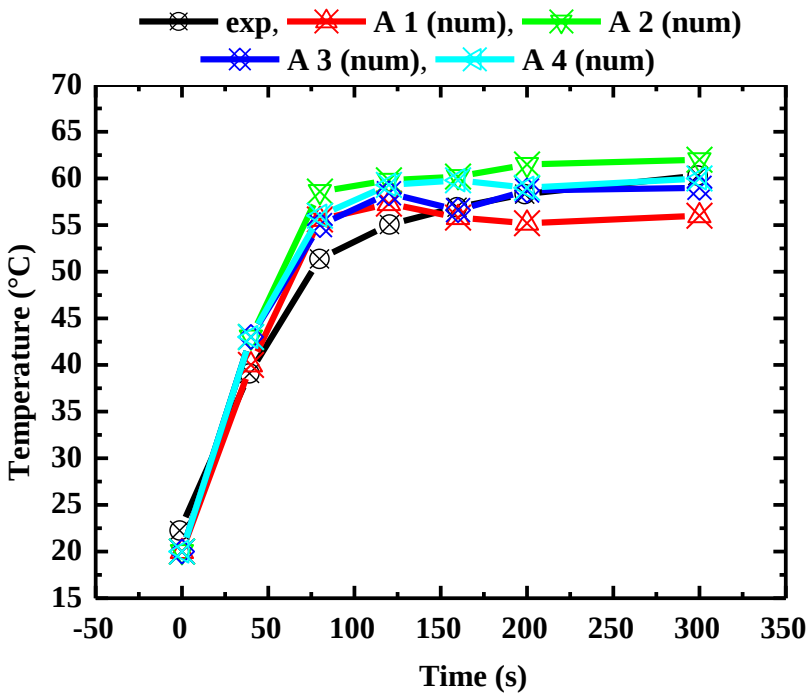

Fig. 3 The temperature distribution as a function of time (measured in the tunnel at 0.85 m height): Curve Validation & Sensitivity on the grid system with 0.2 m (mesh A1), 0.1 m (mesh A2) and 0.187 m (mesh A4).

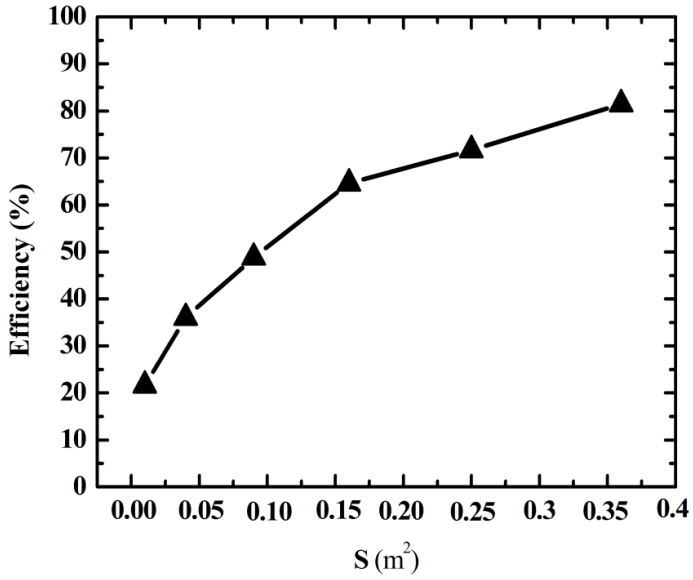

Fig. 4 Duct efficiency for different duct section.

ISSN: 2961-6603

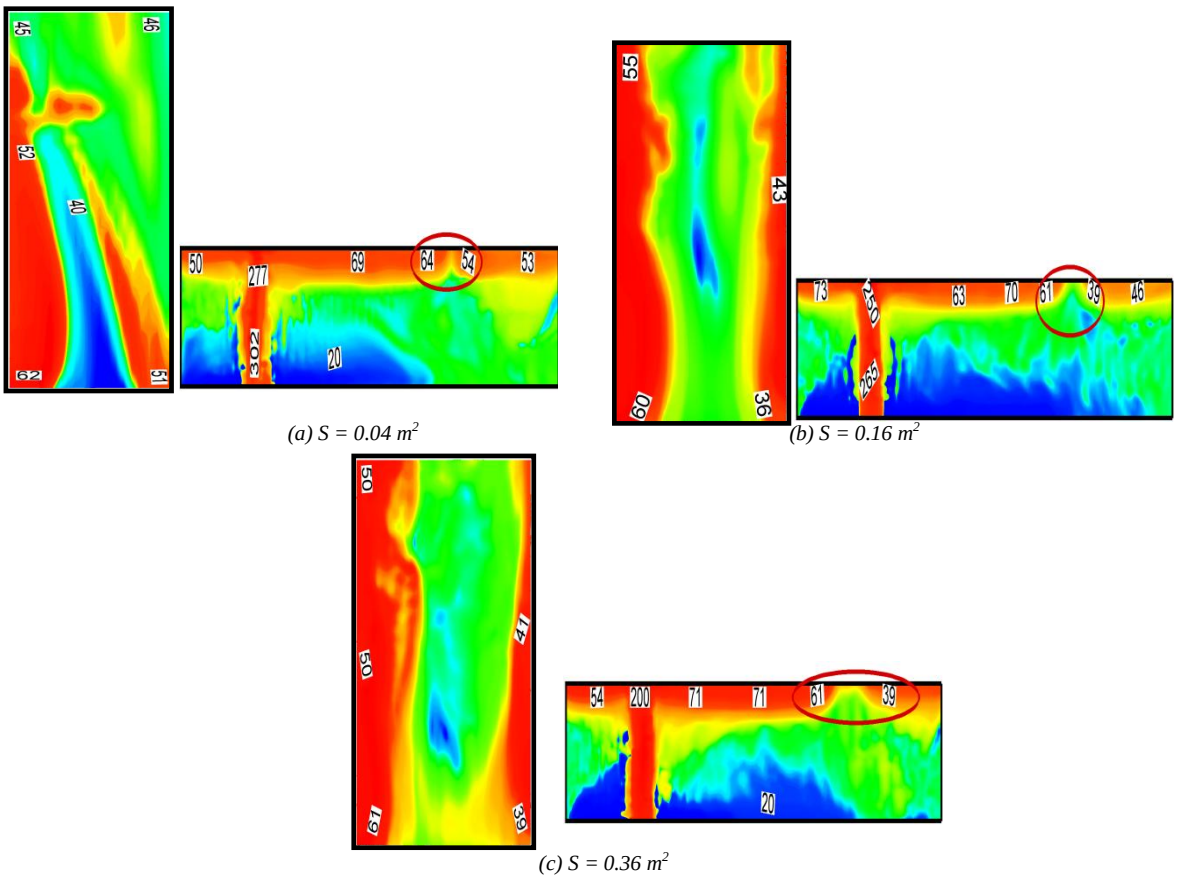

Fig. 5 Temperature Contour distribution for different duct section (5a: S = 0.04m^2, 5b: S = 0.16 m^2, 5c: S = 0.36 m^2) and in the lateral plan XZ (Y = 1) in the corridor (The zone sunken is circulated on red) and in the duct (In the left side: duct system; In the right side: the corridor).

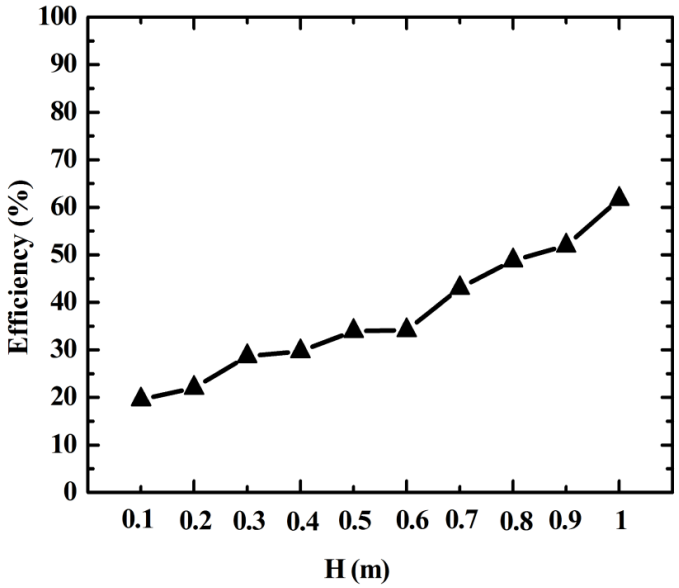

Fig.6 Duct efficiency for different duct height.

ISSN: 2961-6603

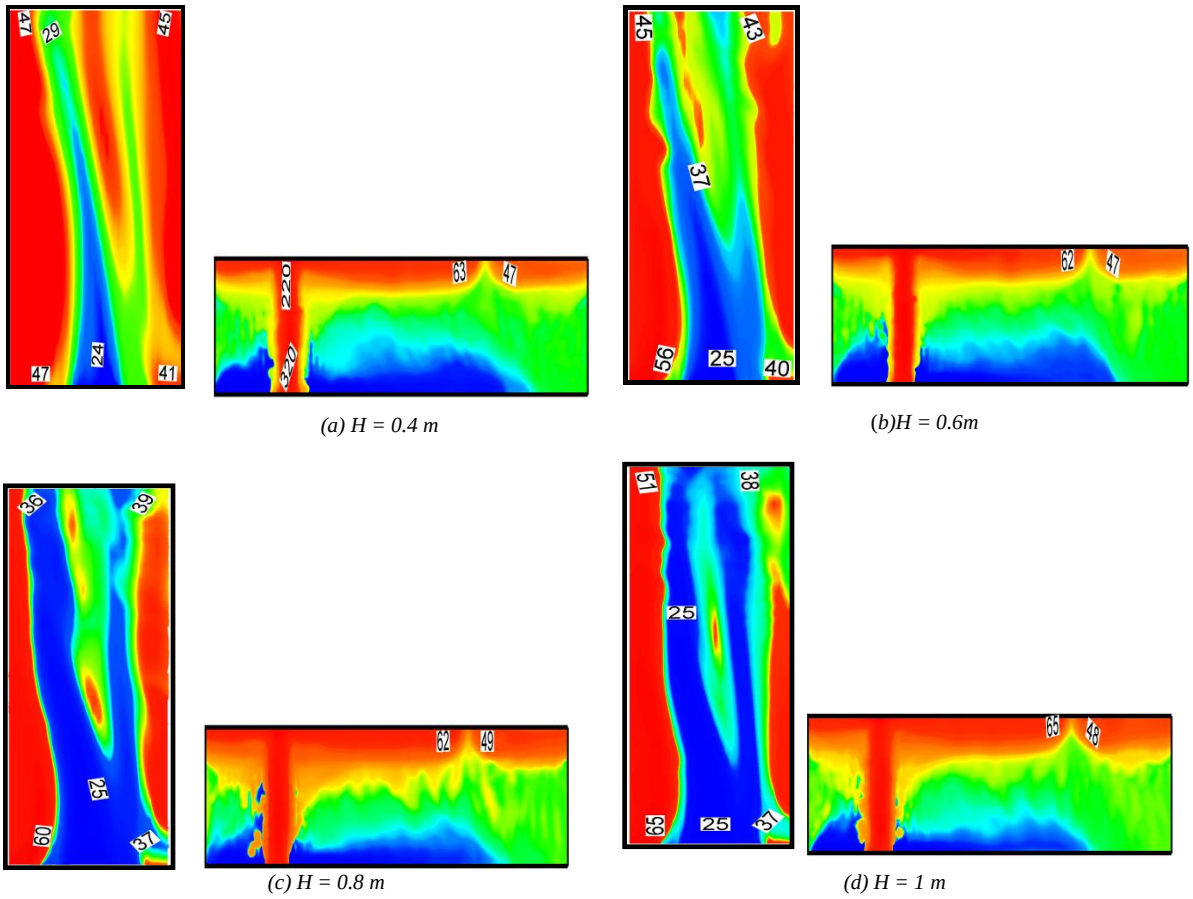

(a) H = 0.4 m (b)*H = 0.6m*

(c) H = 0.8 m *(d) H = 1 m*

Fig. 7 Temperature contour distribution with various duct height (7a: H = 0.4 m,7b: H = 0.6 m, 7c: H = 0.8 m, 7d: H = 1 m) in the corridor and in the duct (In the left side: duct system; In the right side: the corridor).

ISSN: 2961-6603

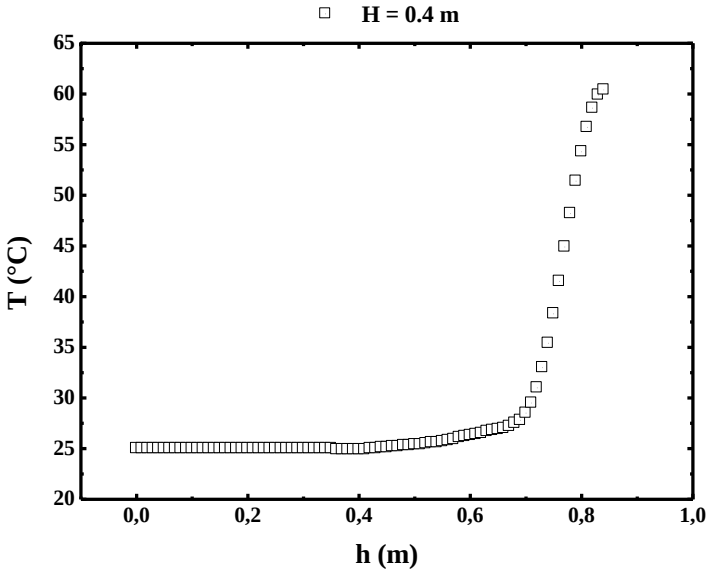

Fig. 8 Temperature distribution as a function of the corridor height: Illustration of the cold and the hot layers.

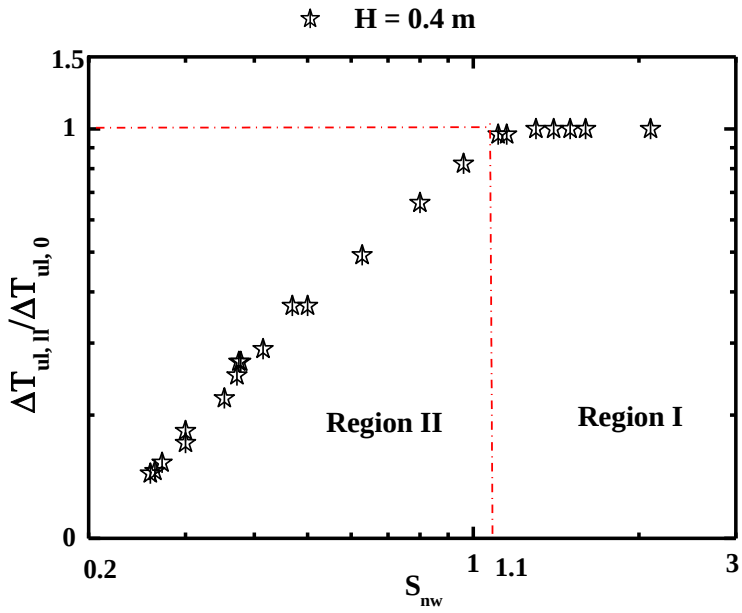

Fig. 9 Thermal stratification with a ceiling duct based on the new parameter $''S_{nw}'$:Illustration of the critical value

ISSN: 2961-6603

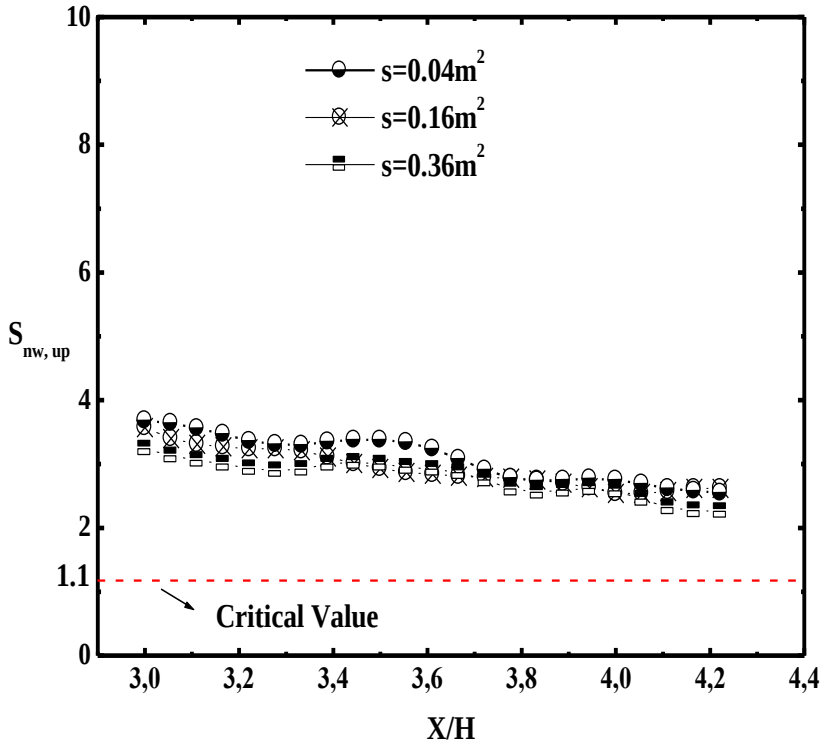

Fig. 10a The upstream evaluation of the new stratification parameter (the new model "S_{nw}") with the duct section variation.

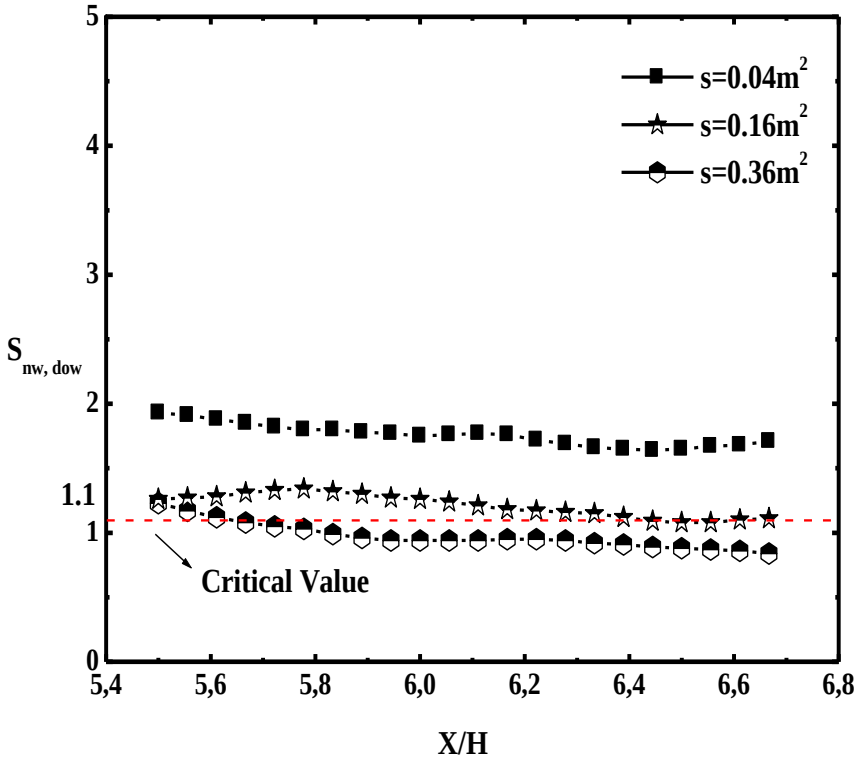

Fig. 10b The downstream evaluation of the new stratification parameter (the new model "S_{nw}") with the duct section variation.

ISSN: 2961-6603

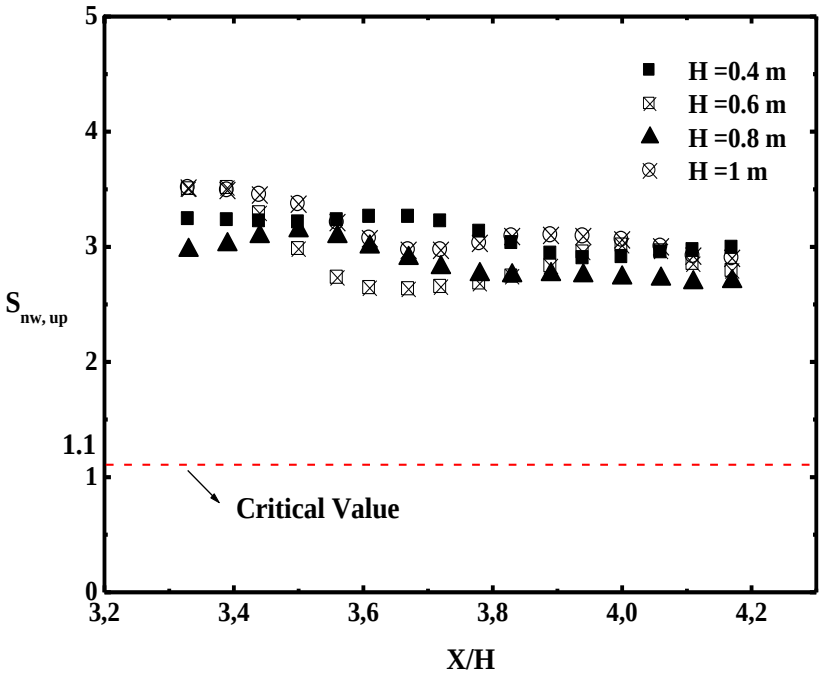

Fig. 11a: The upstream evaluation of the new stratification parameter (the new model "S_{nw}") with the duct height variation.

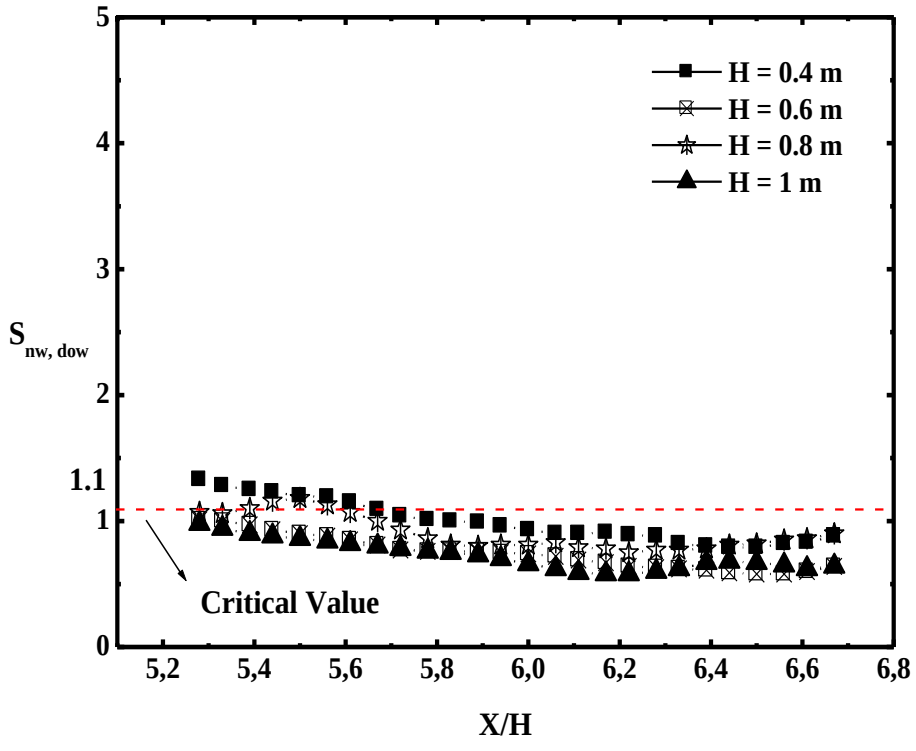

Fig. 11b: The downstream evaluation of the new stratification parameter (the new model "S_{nw}") with the duct height variation.

ISSN: 2961-6603

ACKNOWLEDGMENT

The main manuscript text and the prepared figure are written by Dr. Imen Ben Abdellaziz. Pr. Mourad Bouterra reviewed the manuscript.

REFERENCES

[1] C.H. Yoon, M.S. Kim, J. Kim, "The evaluation of natural ventilation pressure in Korean long road tunnels with vertical shafts," *Tunnelling Underground Space Technol*, vol. 21, pp. 3–4, 2006.

[2] J.F. Mao, J. Zhou, Y.L. Huang, Y.J. Yao, "Experimental study on temperature distribution under fire circumstance in natural ventilation city tunnel," *Refrigeration Air Conditioning & Electric Power Machinery*, vol. 1, pp. 1–4, 2009.

[3] J.Ji, Z.H. Gao, C.G. Fan, W. Zhong, J.H. Sun, "A study of the effect of plug-holing and boundary layer separation on natural ventilation with vertical shaft in urban road Tunnel fires," *Int. J. Heat Mass Transfer*, vol. 55, pp. 6032-6041, 2012.

[4] F. Vuilleumier, A. Weatherill, B. Crausaz, "Safety aspects of railway and road tunnel: example of the Lotschberg railway tunnel and Mont-Blanc road tunnel," *Tunnelling and Underground Space Technology*, vol. 17, pp. 153–158, 2002.

[5] L.F. Chen, L.H. Hu, W. Tang, L. Yi, "Studies on buoyancy driven two-directional smoke flow layering length with combination of point extraction and longitudinal ventilation in tunnel fires," *Fire Saf. J.*, vol. 59, pp. 94-101, 2013.

[6] J.Ji, L. Kaiyuanb, Z. Wei, H. Ran, "Experimental investigation on influence of smoke venting velocity and vent height on mechanical smoke exhaust efficiency," *J. Hazard. Mater*, vol. 177, pp. 209-215, 2010.

[7] C.C Hwang, J.C. Edwards, "The critical ventilation velocity in tunnel fires-a computer simulation," *Fire Saf. J.*, vol. 40, pp. 213-244, 2005.

[8] B. Kalech, Z. Mehrez, M.Bouterra, A. El Cafsi and A. Belghth, "Temperature Stratification in a Road Tunnel," *Thermal Science*, Vol. 20, pp. 223-237, 2016.

[9] O. Vauquelin, O. Mégret, "Smoke extraction experiments in case of fire in a tunnel," *Fire Saf. J*, vol. 37, pp. 525-533, 2002.

[10] J.Ji, J.Y. Han, C.G. Fan, Z.H. Gao, J.H., Sun, "Influence of cross-sectional area and aspect ratio of shaft on natural ventilation in urban road tunnel," *Int. J. Heat Mass Transfer*, vol. 67, pp. 420-431, 2013.

[11] W. Zhong, C.G. Fan, J. Ji, J.P. Yang, "Influence of longitudinal wind on natural ventilation with vertical shaft in a road tunnel fire," *Int. J. Heat Mass Transfer*, vol. 57, pp. 671-678, 2013.

[12] Lu He, Yuyang Ming, Ke Liao, Haojun Zhang, Chenhao Jia, Guoqing Zhu, Haowen Tao, "A study on the Behavior Characteristics of Air Supply during Tunnel Fires under Natural Ventilation with Multiple Vertical Shafts," *Fire*, vol. 6(10), pp. 393, 2023.

[13] F.Tang, L.J.Li, M.S.Dong, Q.Wang, F.Z.Mei, "Characterization of buoyant flow stratification behaviors by Richardson (Froude) number in a tunnel fire with complex combination of longitudinal ventilation and ceiling extraction," *Appl. Therm. Eng.*, vol. 110, pp. 1021-1028, 2017.

[14] Huang, D.F., Li, S.C., "An experimental investigation of stratification characteristic of fire smoke in the corridor under the effect of outdoor wind," *J. Wind Eng. Ind. Aerod*, vol. 179, pp. 173–183, 2018.

[15] A. Mos, B. Gay, "Phenomenological models for fire simulation in road tunnels," thesis, University of Claude Bernard-Lyon, 2005.

[16] K. Mc Grattan, R.M. Dermott, S. Hostikka, J. Floyd, "Fire Dynamics Simulator (version 5)-User's Guide, National Institute of Standards and Technology, Baltimore, Maryland, NIST Special Publication, 1019-5, 2010.

[17] K. Mc Grattan, S. Hostikka, J. Floyd, H. Baum, R. Rehm, W. Mell, R.M. Dermott, "Fire Dynamics Simulator (version 5)-Technical Reference Guide, National Institute of Standards and Technology, Baltimore, Maryland, NIST Special Publication, 1018-5, 2010.

[18] Hu, L. H., et al., "Modeling Fire-Induced Smoke Spread and Carbon Monoxide Transportation in a Long Channel: Fire Dynamics Simulator Comparisons with Measured Data," *J. Hazard. Mater*, vol. 140, pp. 293-298, 2007.

[19] Ying Zhen Li , Bo Lei, and Haukur Ingason, "Scale modeling and numerical simulation of smoke control for rescue stations in long railway tunnels," *Journal of Fire Protection Engineering*, vol. 22(2), pp. 101-131, 2012.

[20] J. Ji, Z.H. Gao, C.G. Fan, J.H. Sun, "Large Eddy Simulation of stack effect on natural smoke exhausting effect in urban road tunnel fires," *Int. J. Heat Mass Transfer*, vol. 66, pp. 531-542, 2013.

[21] J. Smagorinsky, "General circulation experiment with the primitive equations, I. The basic experiment," *Mon. Weather Rev.*, vol. 9, pp. 99-164, 1963.

ISSN: 2961-6603

[22] C.G. Fan, J. Ji, W. Wang, J.H. Sun, "Effects of vertical shaft arrangement on natural ventilation performance during tunnel fires," *Int. J. Heat Mass Transfer*, vol. 73, pp. 158-169, 2014.

[23] J. Ji, C.G. Fan, Z.H. Gao, J.H. Sun, "Effects of vertical shaft geometry on natural ventilation in Urban road tunnel fires," *J Civ Eng Manag.*, vol. 20, pp. 466–476, 2014.

[24] Y.Z. Li, H. Ingason, "Model scale tunnel fire tests with automatic sprinkler," *Fire Saf J*, vol. 61, pp. 298–313, 2013.

[25] N.B. Kaye, G.R. Hunt, "Smoke filling time for a room due to a small fire: the effect of ceiling height to floor width aspect ratio," *Fire Saf J*, vol. 42 (2), pp. 329–339, 2007.

[26] F. Demouge, "Contribution to a numerical modeling of smoke stratification in case of a road tunnel fire,"doctoral thesis, University of Claude Bernard - Lyon 1, 2002.

ISSN: 2961-6603